How to cite: *Angew. Chem. Int. Ed.* **2023**, *62*, e202213686
International Edition: doi.org/10.1002/anie.202213686
German Edition: doi.org/10.1002/ange.202213686

Photoredox Catalysis

# Formyl Radical Generation from α-Chloro *N*-Methoxyphthalimides Enables Selective Aldehyde Synthesis

*Dan Liu[+], Kai Yang[+], Di Fang[+], Shi-Jun Li, Yu Lan,* and Yiyun Chen**

**Abstract:** The aldehydes installation by radical formylation constitutes an attractive synthetic strategy. However, the generation of formyl radicals for organic synthesis applications remains unknown. Herein we report the first formyl radical generation from α-chloro *N*-methoxyphthalimides, which selectively synthesize aldehydes by alkene hydroformylation under mild photoredox conditions. The aldehydes can be installed on acrylates, acrylamides, vinyl sulfones, vinyl ketones, and complex steroids by radical hydroformylation in excellent chemoselectivity and regioselectivity. The concerted hydrochloride elimination for the formyl radical generation from α-chloro methoxy radicals is established by experimental and computational approaches.

Aldehydes widely exist in bioactive molecules and are useful building blocks (Scheme 1a).[1] The transition-metal-catalyzed hydroformylations with syngas (carbon monoxide and hydrogen gas) as formyl metal precursors have found broad synthetic applications.[2,3] N-heterocyclic carbene catalysis achieved the formation of formyl anion equivalents from D-(+)-glucose.[4,5] While effective, the requirement of well-designed ligands for transition-metal-catalyzed hydroformylation and the limited chalcone substrate scope for formyl anion additions call for new reaction manifolds. To this end, radical formylation provides an attractive alternative to formyl metal and formyl anion intermediates. However, there were only isolated reports on formyl radical generation from high-energy irradiation or electrolysis.[6] In those reactions, various parallel reaction pathways were observed. They resulted in no synthetic application, which was in sharp contrast to widely studied acyl radicals with alkyl or aryl substitutions (R≠H, Scheme 1b).[7] Alternatively, the masked formyl radical equivalents were developed, but the acetal group deprotection required strong acid treatment to release the free aldehyde, which was tedious and incompatible with many functional groups.[8]

Kaiser previously reported that short-wavelength UV irradiation on chlorine/oxygen gas generated the chlorine radical, which subsequently abstracted the hydrogen atom

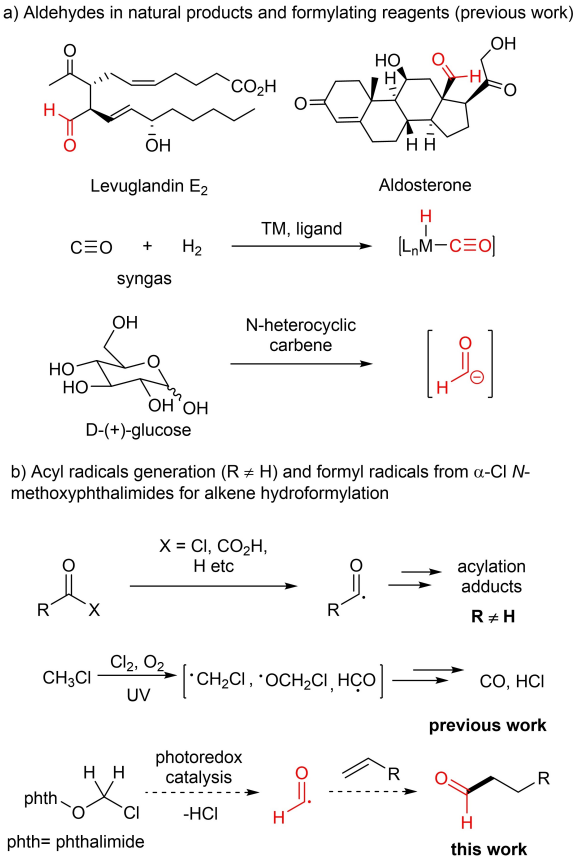


***Scheme 1.*** The aldehyde synthesis and formylating reagents.

[*] D. Liu,[+] D. Fang,[+] Y. Chen
State Key Laboratory of Bioorganic and Natural Products Chemistry, Shanghai Institute of Organic Chemistry, University of Chinese Academy of Sciences, Chinese Academy of Sciences
345 Lingling Road, Shanghai 200032 (China)
E-mail: yiyunchen@sioc.ac.cn

Y. Chen
School of Physical Science and Technology
ShanghaiTech University
100 Haike Road, Shanghai 201210 (China)
and
School of Chemistry and Material Sciences, Hangzhou Institute for Advanced Study, University of Chinese Academy of Sciences
1 Sub-lane Xiangshan, Hangzhou 310024 (China)

K. Yang,[+] S.-J. Li, Y. Lan
Green Catalysis Center, College of Chemistry, Zhengzhou University
Zhengzhou, Henan, 450001 (China)

Y. Lan
School of Chemistry and Chemical Engineering, Chongqing Key Laboratory of Theoretical and Computational Chemistry
Chongqing University
Chongqing 400030 (China)

[+] These authors contributed equally to this work.



© 2022 Wiley-VCH GmbH

15213773, 2023, 1, Downloaded from https://onlinelibrary.wiley.com/doi/10.1002/anie.202213686 by Yiyun Chen - <Shibboleth>-member@sioc.ac.cn , Wiley Online Library on [27/01/2023]. See the Terms and Conditions (https://onlinelibrary.wiley.com/terms-and-conditions) on Wiley Online Library for rules of use; OA articles are governed by the applicable Creative Commons License

from chloromethanes to yield the chloromethyl radical (Scheme 1b).[6f] This chloromethyl radical was further oxidized by oxygen gas to obtain the highly unstable α-chloro methoxy radical and finally transformed into formyl radicals.[6f, 9] However, this approach resulted in only carbon monoxide and hydrochloride formation, which demonstrated no synthetic application. We envision that the new formyl radical generation method under mild conditions may enable the synthetic applications of formyl radicals and accelerate the formyl radical investigations. Based on our previous work on alkoxyl radical generation under mild conditions,[10] we report the first formyl radical generation from bench-stable α-chloro *N*-methoxyphthalimides by photoredox catalysis,[11] enabling the selective aldehydes synthesis.

The one-step synthesis with *N*-hydroxyphthalimides and bromochloromethanes afforded α-chloro *N*-methoxyphthalimide **1** in 71 % yield, which easily scaled up to grams.[12] Then, the possible generation of α-chloro methoxy radicals under photocatalytic conditions was explored with Hantzsch ester (HE) as the reductant and *fac*-Ir(ppy)$_3$ as the photocatalyst. Pleasingly, the benzyl 4-oxobutanoate **3** was obtained in 27 % yield by reacting with acrylate **2** (Table 1, entry 1), which indicated the formyl radical generation. However, it was accompanied by many side products. The change of dioxane solvent to dichloromethane increased **3** to 56 % yield, and acetonitrile gave the optimal 76 % yield of **3** with little side products (72 % isolated yield, entries 2–3, see Schemes S1–S2 for details). The reaction was not sensitive to water, and the air atmosphere only slightly decreased the yield of **3** (Tables S2–3). The addition of sodium bicarbonate did not affect the reaction to afford 70 % yield of **3** (entry 4). The HE and light irradiation were critical for the reaction (entries 5–6). The removal of [Ir] afforded **3** in 41 % yield, presumably by the electron donor-acceptor complex reactivity of HE and *N*-methoxyphthalimides (entry 7, see Figures S5–S7 for details).[11c,13] The reaction was easily scaled up to 2 mmol to afford **3** in 74 % isolated yield (entry 8).

We further prepared α-fluoro *N*-methoxyphthalimide **4** from bromofluoromethane similarly in 87 % yield. In standard reaction conditions, the hydroformylation adduct **3** was obtained in 15 % yield unexpectedly (entry 9), indicating the presumable α-fluoro methoxy radical from **4** may also yield the formyl radical. With the increased equivalents of HE and **4**, we obtained 75 % yield of **3** with sodium bicarbonate additions to facilitate the hydrofluoride elimination (entry 10). The α-methoxy *N*-methoxyphthalimide **5** and α-tertbutoxy *N*-methoxyphthalimide **6** were prepared similarly, and they yielded the hydroformylation adduct **3** in modest 11 % and 33 % yields, respectively (entries 11–12).

We next investigated the substrate scope of hydroformylation with α-chloro *N*-methoxyphthalimides **1** (Scheme 2). Using different acrylate radical acceptors **7b**–**15b**, the sensitive functional groups silyl ethers, terminal

***Table 1:*** Optimization of radical hydroformylation.

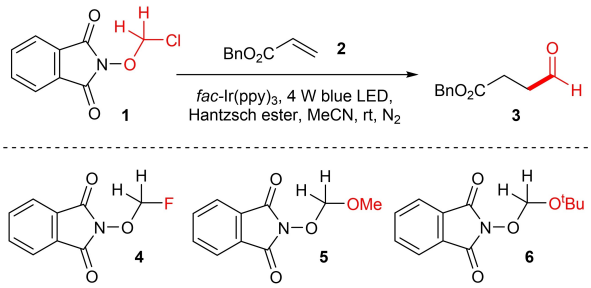


| Entry | Conditions[a] | Conv. of **1** [%][b] | Yield of **3** [%][b] |
|---|---|---|---|
| 1 | **1**, dioxane | 160 | 27 |
| 2 | **1**, DCM | >195 | 56 |
| 3 | **1**, $CH_3CN$ | >195 | 76 (72) |
| 4 | **1**, 2.0 eq. $NaHCO_3$ | >195 | 70 |
| 5 | Entry 3, no HE, 3 h | <5 | <5 |
| 6 | Entry 3, no light, 3 h | <5 | <5 |
| 7 | Entry 3, no [Ir], 3 h | >195 | 41 |
| 8 | Entry 3[c] | >195 | (74) |
| 9 | **4**, $CH_3CN$ | 140 | 15 |
| 10[d] | Entry 9, 2.0 eq. $NaHCO_3$ | 170 | 75 |
| 11 | **5**, $CH_3CN$ | 52 | 11 |
| 12 | **6**, $CH_3CN$ | 132 | 33 |

[a] Reaction conditions: **1** (0.20 mmol, 2.0 equiv), **2** (0.10 mmol, 1.0 equiv), *fac*-Ir(ppy)$_3$ (0.001 mmol, 1 mol %) and Hantzsch ester (0.30 mmol, 3.0 equiv) in 2.0 mL MeCN under nitrogen with 4 W blue LED irradiation at ambient temperature for 1 h, unless otherwise noted. [b] Conversion and yields were determined by $^1$H NMR analysis and isolated yields were in parentheses. [c] 2 mmol of **2**. [d] 5.0 equiv **4** and 5.0 equiv HE was used.

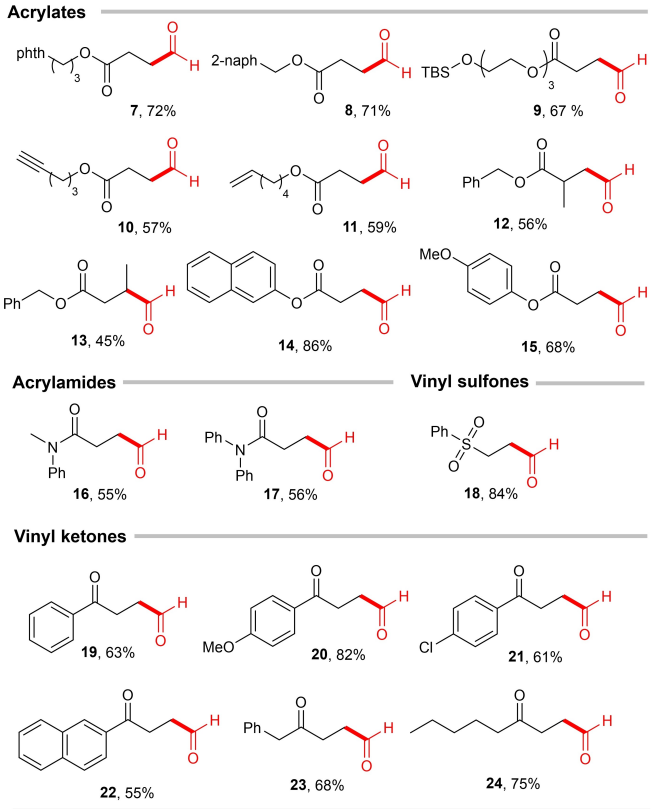


***Scheme 2.*** Substrate scope of hydroformylation. Reaction conditions: entry 3 in Table 1. Isolated yields.



© 2022 Wiley-VCH GmbH

15213773, 2023, 1, Downloaded from https://onlinelibrary.wiley.com/doi/10.1002/anie.202213686 by Yiyun Chen - <Shibboleth>-member@sioc.ac.cn , Wiley Online Library on [27/01/2023]. See the Terms and Conditions (https://onlinelibrary.wiley.com/terms-and-conditions) on Wiley Online Library for rules of use; OA articles are governed by the applicable Creative Commons License

alkynes, and terminal alkenes were all tolerated to afford 4-oxobutanoates **7**–**15** in 45–86 % yields, which provided the complementary functional group compatibility with transition-metal-catalysis.[14,8a] Among acrylates, the phenol acrylates **14b**–**15b** gave superior 68–86 % yields. The α-disubstituted and β-substituted acrylates **12b** and **13b** also reacted to give **12** and **13** in slightly decreased 45–56 % yields. The acrylamides **16b**–**17b** afforded 4-oxobutanamides **16**–**17** in 55–56 % yields. Vinyl sulfone **18b** reacted smoothly to yield 3-sulfonylaldehydes **18** in an excellent 84 % yield. Various vinyl ketones **19b**–**24b** with alkyl or aryl substitutions were suitable radical acceptors to obtain 4-ketoaldehydes **19**–**24** in 55–82 % yields. These alkene substrate scopes include acrylates, acrylamides, vinyl sulfones, and vinyl ketones, which are far beyond the state-of-the-art formyl anion addition reaction for hydroformylation and may find broad applications in aldehyde synthesis.[5]

The reaction was next probed by mechanistic investigations (Scheme 3). From redox potential measurements, the reduction potentials of **1**, **4**, **5**, and **6** with different α-substituents all fell in the oxidation potential range of *fac*-Ir(ppy)$_3$(II) for the single-electron reduction (see Figures S8–14). Similarly, the α-chloro *N*-methoxybenzotriazole **25** afforded **3** in 42 % yield with the reduction potential $E_p = -0.13$ V vs SCE in MeCN.[15] Fluorescence quenching experiments indicated that Hantzsch ester quenched the excited *fac*-Ir(ppy)$_3$ more effectively than **1** and **2** (Figures S15–S17). We then explored the possible formaldehyde intermediate in the reaction conditions to generate the formyl radical via the intermolecular HAT pathway.[16] In the crossover experiments with benzaldehydes **26** and **1**, only the formyl radical addition product **3** was observed in 70 % yield (Scheme 3b). In contrast, the benzoyl radical addition product **27** from benzaldehydes **26** was not observed, which excluded the intermolecular HAT pathway.[11a, 17]

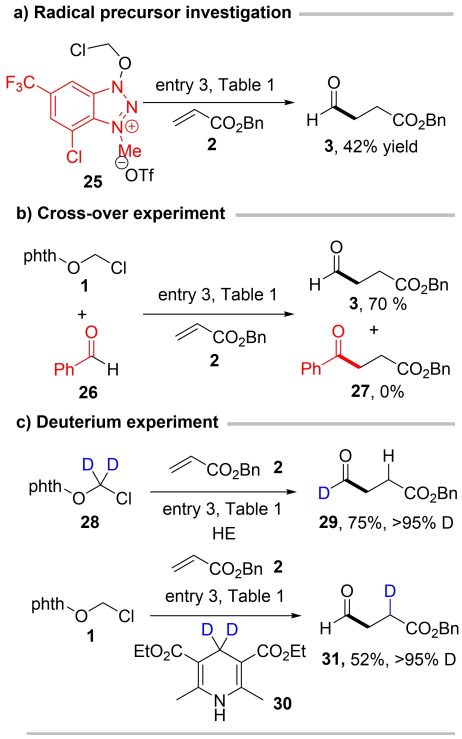


***Scheme 3.*** Mechanistic investigations.

We also prepared the deuterated α-chloro *N*-methoxyphthalimide **28**, which afforded the deuterated **29** in 75 % yield with the exclusive deuterium incorporation at the aldehyde (Scheme 3c). With the deuterated Hantzsch ester **30**, the deutylformylation adduct **31** was obtained in 52 % yield with >95 % α-D incorporation, whereas the deuteration at the aldehyde was not observed. When the N–D Hantzsch ester or the deuterated water was used, the reaction was unaffected and the deutylformylation product was not obtained (Schemes S5–S6). These results suggested the hydroformylation attributed to the HAT instead of the protonation, and the formyl anion was unlikely to exist.[18] The quantum yield of the reaction was 7.0 and suggested the chain reaction pathway (Figure S20).

Based on our experimental observations,[19] we envision the formyl radical generation from α-chloro methoxy radical is worthy of further investigations as a fundamental process. To this end, the density-functional theory (DFT) calculations at M06-2X/6-31G(d)/IEF-PCM$_{(MeCN)}$ level were employed (computational details are given in Supporting Information). The spin density of chloromethoxy radical **32** was exhibited to locate on the oxygen atom (0.907), which may drive further fragmentation by inducing the C–Cl bond cleavage (Figure S2). Based on this observation, possible transition states were visualized by the DFT calculation. As shown in Scheme 4a, the geminal elimination of HCl occurs via the transition state **33ts** with a free energy barrier of 12.7 kcal mol$^{-1}$. Afterward, the formyl radical **34** is formed through the concerted pathway with an exergonic energy of 7.7 kcal mol$^{-1}$ (red lines). In the alternative stepwise pathway, the C–Cl bond cleavage occurs via the transition state **37ts** with a free energy barrier of 15.0 kcal mol$^{-1}$ (blue lines). Afterward, the free Cl radical reacts with the formaldehyde intermediate **38** through a hydrogen atom transfer transition state **39ts** to provide the formyl radical **34**. The C–H bond cleavage through the transition state **40ts** and 1,2-hydrogen atom shift through the transition state **35ts** were also considered.[11d,e] However, those pathways were easily excluded by the prohibitory high activation free energy.

The C–Cl bond lengths in the transition state **33ts** and **37ts** showed the similar numbers as 2.267 Å and 2.230 Å, which suggested the C–Cl bond vibration orientation may determine the reaction mechanism (Scheme 4b). We next carried out quantum dynamics simulations at the M06-2X/6-31G(d)/IEF-PCM$_{(MeCN)}$ level using the quantum trajectory mean-field (QTMF) program interfaced with Gaussian 09.[20,21] The 2D projected map of quantum dynamics for Cl–H and C–Cl distances was shown in Scheme 4c, which calculated twenty trajectories starting from the ground state of chloromethoxy radical **32** (Figure S4 for details). These trajectories show that chloromethoxy radicals remain in the stretching vibration region for most of the duration. When the stretching vibration of the C–Cl bond reaches to a certain extent, this bond tends to break. In sixteen of twenty


© 2022 Wiley-VCH GmbH

15213773, 2023, 1, Downloaded from https://onlinelibrary.wiley.com/doi/10.1002/anie.202213686 by Yyun Chen - <Shibboleth>-member@sioc.ac.cn , Wiley Online Library on [27/01/2023]. See the Terms and Conditions (https://onlinelibrary.wiley.com/terms-and-conditions) on Wiley Online Library for rules of use; OA articles are governed by the applicable Creative Commons License

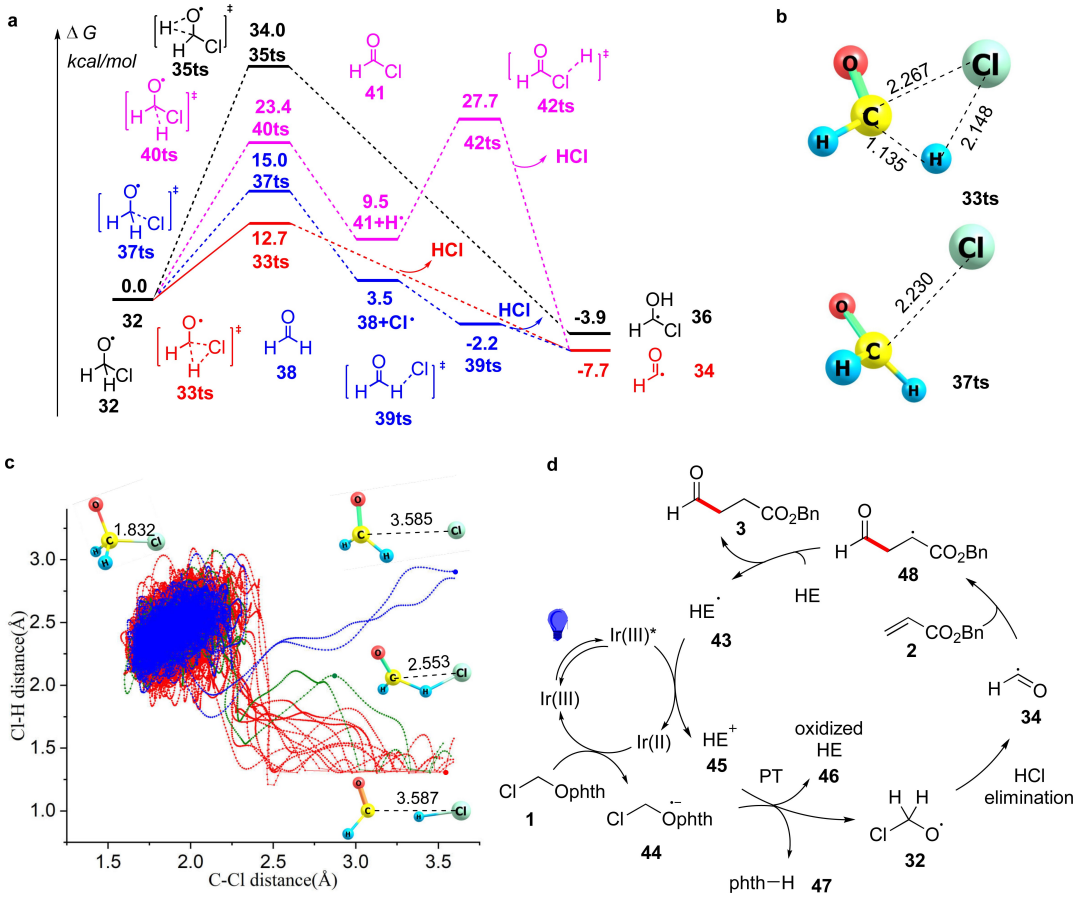


***Scheme 4.*** Computational studies and mechanistic proposal. a) Free energy profile for the formation of formyl radical. b) The 3D structures for **33ts** and **37ts** (distance Å). c) The 2D projected map of quantum dynamic studies. d) Proposed reaction mechanism.

trajectories, the elongation of C–Cl bond and the cleavage of C–H bond occur simultaneously to allow for the concerted reaction pathway (red lines, see the example trajectory video in the Supporting Information). Only two trajectories showed the stepwise pathway by a direct C–Cl bond cleavage with the Cl radical elimination (blue lines, see the example trajectory video in the Supporting Information). Interestingly, two trajectories indicated the semi-concerted pathway, which showed the reaction initiation from the C–Cl bond cleavage accompanied by the formaldehyde hydrogen atom abstraction from the Cl radical (green lines, see the example trajectory video in the Supporting Information). To sum up, the concerted elimination from the chloromethoxy radical is the favorable main reaction pathway. However, the stepwise and semi-concerted pathways cannot be completely excluded.

Based on the experimental and computational investigations above, the reaction mechanism for the radical formylation is proposed in Scheme 4d. The excited photocatalyst $Ir^{III}$* is reduced by the Hantzsch ester (HE) radical **43** to afford the $Ir^{II}$ species. The chloro *N*-methoxyphthalimide substrate **1** reacts with $Ir^{II}$ by single electron transfer (SET) to obtain the anionic radical **44**, which further undergoes proton transfer with **45** to release the α-chloroalkoxy radical **32**, phthalimide **47**, and oxidized HE **46**. α-Chloroalkoxy radical **32** undergoes the HCl geminal elimination to provide the formyl radical **34**, which then adds to electron-deficient alkenes **2** to afford the alkyl radical **48**. The HAT by HE yields the hydroformylation product **3** with the HE radical **43** regeneration.

We further explored the distinction between the geminal elimination of α-chloroalkoxy radicals with the β-fragmentation of alkoxy radicals (Scheme 5a). The α-acetyl *N*-methoxyphthalimide **49** underwent β-fragmentation in the standard conditions to obtain the acetyl radical, which further yielded the hydroacetylation adduct **50** in 72 % yield with acrylate **2**.[22] However, the α-formyl *N*-methoxyphthalimide **51** failed to yield the formyl radical and only afforded <5 % yield of the hydroformylation adduct **3**. In contrast, the α-chloro *N*-acetoxyphthalimide **52** afforded the acetyl radical from the α-chloro ethoxy radical by the geminal elimination under the standard reaction conditions, and it further reacted with acrylate **2** to afford **50** in 70 % yield. These results highlighted the unique reactivity of formyl radicals compared to other acyl radicals and explained the lack of previous reports on the formyl radical generation from β-fragmentation.

We next investigated if the geminal elimination of α-substituted alkoxy radicals could go beyond the hydrochloride elimination. The α-fluoro *N*-ethyl glycolate


© 2022 Wiley-VCH GmbH

15213773, 2023, 1, Downloaded from https://onlinelibrary.wiley.com/doi/10.1002/anie.202213686 by Yyun Chen - <Shibboleth>-member@sioc.ac.cn , Wiley Online Library on [27/01/2023]. See the Terms and Conditions (https://onlinelibrary.wiley.com/terms-and-conditions) on Wiley Online Library for rules of use; OA articles are governed by the applicable Creative Commons License

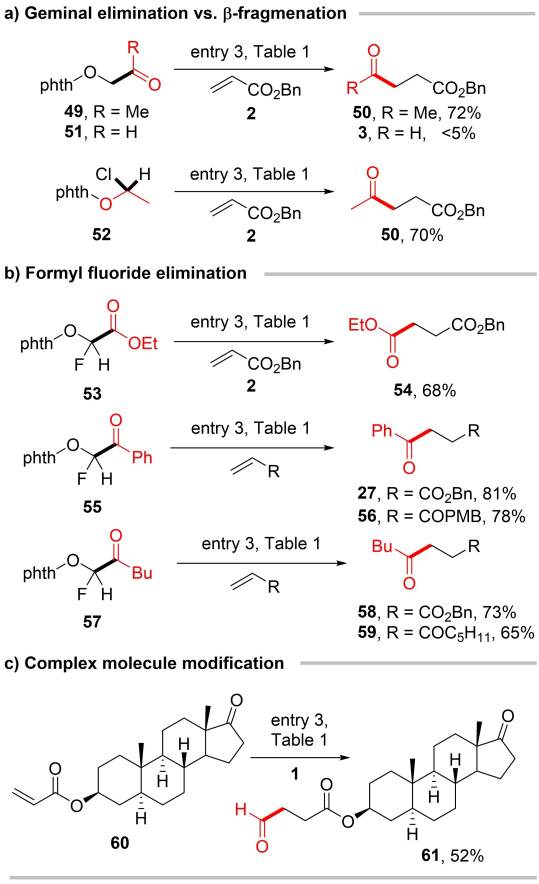


***Scheme 5.*** Geminal elimination and β-fragmentation of alkoxyl radicals.

phthalimide **53** was prepared in one step in gram scales and subjected to the standard reaction conditions (Scheme 5b). Hypothetically, the α-fluoro alkoxyl radical from **53** may undergo the sequential hydrofluoride elimination and carbon monoxide release (a formally formyl fluoride elimination) to yield the ethyl formate radical. Indeed, the hydroesterification adduct **54** was observed in 68 % yield with acrylate **2**. This sequential elimination easily extended to acyl radical generation with aryl or aliphatic substitutions from **55** and **57** to afford the corresponding hydroacylation adducts in excellent 65–81 % yields. The complex steroid-derived **60** underwent hydroformylation selectively to afford **61** with the unprotected aldehyde installation in 52 % yield, and those functional groups on the steroid were unaffected (Scheme 5c).

In conclusion, we reported the first selective aldehyde synthesis via radical hydroformylation, enabled by the formyl radical generation from α-chloro *N*-methoxyphthalimides under mild photoredox conditions. The experimental and theoretical investigations, including molecular dynamics studies, validated the concerted hydrochloride elimination from α-chloro methoxy radicals. The unprotected aldehydes can be quickly introduced to complex steroid-derived molecules with excellent chemoselectivity and regioselectivity. We envision this new formyl radical generation method may inspire its reactivity discovery for synthetic applications under mild conditions.

## Acknowledgements

Financial support was provided by the National Natural Science Foundation of China 91753126, 21622207, CAS Interdisciplinary Innovation Team JCTD-2020-16, Program of Shanghai Academic/Technology Research Leader 21XD1424700, Strategic Priority Research Program of the Chinese Academy of Sciences XDB20020200, Program for Science Technology Innovation Talents in Universities of Henan Province (No. 20HASTIT004), and National Supercomputing Center in Zhengzhou.

## Conflict of Interest

The authors declare no conflict of interest.

## Data Availability Statement

The data that support the findings of this study are available in the supplementary material of this article.

**Keywords:** Aldehydes · Alkoxy Radical · Density-Functional Calculations · Formyl Radical

[1] E. V. Gusevskaya, J. Jiménez-Pinto, A. Börner, *ChemCatChem* **2014**, *6*, 382–411.
[2] a) R. Franke, D. Selent, A. Borner, *Chem. Rev.* **2012**, *112*, 5675–5732; b) J. Pospech, I. Fleischer, R. Franke, S. Buchholz, M. Beller, *Angew. Chem. Int. Ed.* **2013**, *52*, 2852–2872; *Angew. Chem.* **2013**, *125*, 2922–2944.
[3] M. Vilches-Herrera, L. Domke, A. Börner, *ACS Catal.* **2014**, *4*, 1706–1724.
[4] H. Stetter, *Angew. Chem. Int. Ed. Engl.* **1976**, *15*, 639–647; *Angew. Chem.* **1976**, *88*, 695–704.
[5] a) J. Zhang, C. Xing, B. Tiwari, Y. R. Chi, *J. Am. Chem. Soc.* **2013**, *135*, 8113–8116; b) M. Fleige, F. Glorius, *Chem. Eur. J.* **2017**, *23*, 10773–10776.
[6] a) J. G. Calvert, *J. Chem. Phys.* **1958**, *29*, 954–955; b) J. E. Baggott, H. M. Frey, P. D. Lightfoot, R. Walsh, *Chem. Phys. Lett.* **1986**, *132*, 225–230; c) J. E. Baggott, H. M. Frey, P. D. Lightfoot, R. Walsh, *J. Phys. Chem.* **1987**, *91*, 3386–3393; d) S. K. Jensen, S. R. Keiding, J. Thogersen, *Phys. Chem. Chem. Phys.* **2010**, *12*, 8926–8933; e) N. A. Bauer, E. Hoque, M. Wolf, K. Kleigrewe, T. Hofmann, *Free Radical Biol. Med.* **2018**, *116*, 129–133; f) E. W. Kaiser, T. J. Wallington, *J. Phys. Chem.* **1994**, *98*, 5679–5685.
[7] a) C. Chatgilialoglu, D. Crich, M. Komatsu, I. Ryu, *Chem. Rev.* **1999**, *99*, 1991–2070; b) V. Chudasama, R. J. Fitzmaurice, S. Caddick, *Nat. Chem.* **2010**, *2*, 592–596; c) X. Zhang, D. W. C. MacMillan, *J. Am. Chem. Soc.* **2017**, *139*, 11353–11356; d) M. Zhang, J. Xie, C. Zhu, *Nat. Commun.* **2018**, *9*, 3517; e) E. Voutyritsa, C. G. Kokotos, *Angew. Chem. Int. Ed.* **2020**, *59*, 1735–1741; *Angew. Chem.* **2020**, *132*, 1752–1758; f) B. Budai, A. Leclair, Q. Wang, J. Zhu, *Angew. Chem. Int. Ed.* **2019**, *58*, 10305–10309; *Angew. Chem.* **2019**, *131*, 10411–10415.


© 2022 Wiley-VCH GmbH

15213773, 2023, 1, Downloaded from https://onlinelibrary.wiley.com/doi/10.1002/anie.202213686 by Yiyun Chen - <Shibboleth>-member@sioc.ac.cn , Wiley Online Library on [27/01/2023]. See the Terms and Conditions (https://onlinelibrary.wiley.com/terms-and-conditions) on Wiley Online Library for rules of use; OA articles are governed by the applicable Creative Commons License

[8] a) H. Huang, C. Yu, Y. Zhang, Y. Zhang, P. S. Mariano, W. Wang, *J. Am. Chem. Soc.* **2017**, *139*, 9799–9802; b) S. Zhang, Z. Tan, H. Zhang, J. Liu, W. Xu, K. Xu, *Chem. Commun.* **2017**, *53*, 11642–11645; c) W. Ou, G. Zhang, J. Wu, C. Su, *ACS Catal.* **2019**, *9*, 5178–5183.
[9] a) G. S. Tyndall, T. J. Wallington, M. D. Hurley, W. F. Schneider, *J. Phys. Chem.* **1993**, *97*, 1576–1582; b) S.-K. Wang, Q.-Z. Zhang, H. Hou, B. Wang, F.-X. Liu, Y.-S. Gu, *Chin. J. Chem.* **2001**, *19*, 729–732.
[10] a) K. Jia, Y. Chen, *Chem. Commun.* **2018**, *54*, 6105–6112; b) L. Capaldo, D. Ravelli, *Chem. Commun.* **2019**, *55*, 3029–3032; c) E. Tsui, H. Wang, R. R. Knowles, *Chem. Sci.* **2020**, *11*, 11124–11141; d) L. Chang, Q. An, L. Duan, K. Feng, Z. Zuo, *Chem. Rev.* **2022**, *122*, 2429–2486.
[11] a) J. Zhang, Y. Li, F. Zhang, C. Hu, Y. Chen, *Angew. Chem. Int. Ed.* **2016**, *55*, 1872–1875; *Angew. Chem.* **2016**, *128*, 1904–1907; b) C. Wang, K. Harms, E. Meggers, *Angew. Chem. Int. Ed.* **2016**, *55*, 13495–13498; *Angew. Chem.* **2016**, *128*, 13693–13696; c) J. Zhang, Y. Li, R. Xu, Y. Chen, *Angew. Chem. Int. Ed.* **2017**, *56*, 12619–12623; *Angew. Chem.* **2017**, *129*, 12793–12797; d) J. Zhang, D. Liu, S. Liu, Y. Ge, Y. Lan, Y. Chen, *iScience* **2020**, *23*, 100755; e) Y. Chen, D. Liu, J. Zhang, *Synlett* **2021**, *32*, 356–361.
[12] A. Calder, A. R. Forrester, R. H. Thomson, *J. Chem. Soc. C* **1969**, 512–517.
[13] J. L. Shi, Z. Wang, R. Zhang, Y. Wang, J. Wang, *Chem. Eur. J.* **2019**, *25*, 8992–8995.
[14] H. Huang, X. Li, C. Yu, Y. Zhang, P. S. Mariano, W. Wang, *Angew. Chem. Int. Ed.* **2017**, *56*, 1500–1505; *Angew. Chem.* **2017**, *129*, 1522–1527.
[15] W. Zheng, J. W. Lee, C. A. Morales-Rivera, P. Liu, M. Y. Ngai, *Angew. Chem. Int. Ed.* **2018**, *57*, 13795–13799; *Angew. Chem.* **2018**, *130*, 13991–13995.
[16] Similarly, neither acetyl chlorides nor acetaldehydes was observed in the reaction of *N*-acetoxylphthalimide **52**.
[17] The TEMPO addition inhibited the reaction (Schemes S7–S9). However, the formyl radical trapping adducts could not be observed due to the highly unstable characters of formyl radicals, see refs. [6d, 6e].
[18] L. Pitzer, J. L. Schwarz, F. Glorius, *Chem. Sci.* **2019**, *10*, 8285–8291.
[19] F. Wu, R. W. Carr, *J. Phys. Chem. A* **2002**, *106*, 5832–5840.
[20] B. Xie, L. Liu, G. Cui, W. H. Fang, J. Cao, W. Feng, X. Q. Li, *J. Chem. Phys.* **2015**, *143*, 194107–194119.
[21] B. Xie, G. Cui, W. H. Fang, *J. Chem. Theory Comput.* **2017**, *13*, 2717–2729.
[22] K. Jia, Y. Pan, Y. Chen, *Angew. Chem. Int. Ed.* **2017**, *56*, 2478–2481; *Angew. Chem.* **2017**, *129*, 2518–2521.

Manuscript received: September 16, 2022
Accepted manuscript online: November 7, 2022
Version of record online: November 29, 2022


© 2022 Wiley-VCH GmbH

15213773, 2023, 1, Downloaded from https://onlinelibrary.wiley.com/doi/10.1002/anie.202213686 by Yiyun Chen - <Shibboleth>-member@sioc.ac.cn , Wiley Online Library on [27/01/2023]. See the Terms and Conditions (https://onlinelibrary.wiley.com/terms-and-conditions) on Wiley Online Library for rules of use; OA articles are governed by the applicable Creative Commons License